

Exotic Mott phases of the extended t - J model on the checkerboard lattice at commensurate densities

Didier Poilblanc^{1,2}

¹*Laboratoire de Physique Théorique, C.N.R.S. & Université de Toulouse, F-31062 Toulouse, France*

²*Theoretische Physik, ETH Zürich, CH-8093 Zürich, Switzerland*

(Dated: September 11, 2021)

Coulomb repulsion between electrons moving on a frustrated lattice can give rise, at simple commensurate electronic densities, to exotic insulating phases of matter. Such a phenomenon is illustrated using an extended t - J model on a planar pyrochlore lattice for which the work on the quarter-filled case [cond-mat/0702367] is complemented and extended to $1/8$ - and $3/8$ -fillings. The location of the metal-insulator transition as a function of the Coulomb repulsion is shown to depend strongly on the sign of the hopping. Quite generally, the metal-insulator transition is characterized by lattice symmetry breaking but the nature of the insulating Mott state is more complex than a simple Charge Density Wave. Indeed, in the limit of large Coulomb repulsion, the physics can be described in the framework of (extended) quantum fully-packed loop or dimer models carrying extra spin degrees of freedom. Various diagonal and off-diagonal plaquette correlation functions are computed and the low-energy spectra are analyzed in details in order to characterize the nature of the insulating phases. We provide evidence that, as for an electronic density of $n=1/2$ (quarter-filling), the system at $n = 1/4$ or $n = 3/4$ exhibits also plaquette order by forming a (lattice rotationally-invariant) Resonating-Singlet-Pair Crystal, although with a quadrupling of the lattice unit cell (instead of a doubling for $n = 1/2$) and a 4-fold degenerate ground state. Interestingly, qualitative differences with the bosonic analog (e.g. known to exhibit columnar order at $n=1/4$) emphasize the important role of the spin degrees of freedom in e.g. stabilizing plaquette phases w.r.t. rotational symmetry-breaking phases.

PACS numbers: 75.10.-b, 75.10.Jm, 75.40.Mg, 74.20.Mn, 71.10.Fd

A. Introduction

Frustrating antiferromagnetic (AF) interaction in quantum magnets¹ can give rise to various exotic spin gapped quantum disordered phases which could be realized in a number of fascinating materials such as Kagome, spinels or pyrochlore materials. Among these phases, a Valence Bond Crystal (VBC), the so-called “plaquette phase”, which spontaneously breaks lattice symmetry (while preserving rotation symmetry), is of particular interest and has been identified² in e.g. the Heisenberg model on the checkerboard lattice, a two-dimensional (2D) lattice of corner sharing tetrahedra (i.e. the 2D analog of the three-dimensional pyrochlore lattice as shown in Fig. 1).

Sofar, itinerant correlated fermions on frustrated lattices have been poorly explored and most investigations deal with weakly doped Mott insulators³. A bit more is known for bosonic systems (which can be mapped on quantum spins under magnetic field) for which a larger set of numerical techniques is available (like Quantum Monte Carlo, QMC). On the triangular lattice, hard-core bosons with nearest-neighbor (NN) repulsive interaction exhibit a rich phase diagram⁴ with charge ordering at commensurate $1/3$ or $2/3$ fillings as well as a supersolid (i.e. a phase with both superfluid and charge orders) under light doping. Recently, hard-core bosons with NN repulsion have also been investigated on the checkerboard lattice at $1/4$ -filling where a weakly first-order superfluid-insulator transition has been detected when increasing

Coulomb repulsion⁵. Interestingly, in the large repulsion insulating phase, evidences have been found in favor of lattice symmetry breaking associated to *plaquette ordering* similar to the one of the Quantum Dimer Model (QDM) on the square lattice⁶. A similar plaquette phase has also been identified at half-filling in the same model and on the same lattice using an effective Hamiltonian valid at large repulsion⁷. Such a fascinating behavior is in fact due to the *partial* particle localization occurring via “ice-rule”-like constraints enforced by the minimization of the global Coulomb energy, a “classical” frustrated minimization problem. It is crucial here that such constraints preserve a macroscopic degeneracy of the classical configuration manifold. Indeed, for quarter-filling the Hilbert space is given by the ensemble of fully packed *dimer* coverings (as for the QDM, see Ref. 6) and a fully packed *loop* representation holds at half-filling⁸. Quantum fluctuations which occur within these subspaces via second-order kinetic processes can subsequently lead to exotic symmetry-breaking states. Here the basic ingredient is the interplay between the frustrated nature of the lattice and the Coulomb repulsion (the Ising interaction in the “spin language”).

The investigation of the fermionic analog, i.e. fermions moving on frustrated lattices and subject to (short range) Coulomb repulsion at commensurate densities, is more involved due the famous “fermion sign problem” that prohibits large scale QMC simulations. However, limited progress have been made recently thanks to the construction of effective models describing the low-energy

physics at large Coulomb repulsion. These models (or simple extensions of them) might have known GS in some very special limits (analogous to the Rokhsar-Kivelson point of Ref. 6) and, otherwise, are tractable by weak coupling expansion around a periodic pattern of appropriately chosen clusters⁹ and by Exact Diagonalisation (ED) techniques. In the case of spinless fermions on the checkerboard lattice, the dynamics within the constrained Hilbert space is introduced via 6-sites ring processes on hexagons involving 3 particles simultaneously and gives rise to a rich phase diagram¹⁰ and, under some conditions, to particle fractionalization¹¹. The case of spinful fermions which has been recently investigated at and around quarter-filling¹² involves a second-order kinetic process on the “empty squares” (i.e. the void plaquettes) of the planar pyrochlore lattice. Interestingly, it was shown that the quarter-filled GS is a new type of plaquette insulating phase, the Resonant Singlet Pair Crystal (RSPC): qualitatively, within a given sublattice of the empty squares (the empty squares of the checkerboard lattice of Fig. 1 being decomposed into a “checkerboard” pattern of two sublattices), electron singlet pairs formed on the square diagonals resonate between the two possible configurations. It was shown that such a plaquette phase is remarkably robust w.r.t. perturbations (like diagonal empty square repulsion) contrary to the bosonic case discussed earlier for which a plaquette phase also exists but with a much more limited extension in parameter-space. In addition, it has been argued that lattice symmetry breaking would survive under light doping in the hole-paired region, giving rise to a fermionic analog of a supersolid⁴. It should be noticed that, besides electronic systems on frustrated lattices with large Coulomb interactions, cold atoms in optical lattices offer also a fantastic playground for such ideas since models of the form discussed in this paper can in principle be realized by the appropriate tuning of atomic interactions¹³.

In this paper, we largely extend the investigation of correlated fermions on the checkerboard lattice initiated in Ref. 12 by considering, besides $n = 1/2$ (quarter-filling), other electron fillings like $n = 1/4$ (1/8-filling) and $n = 3/4$ (3/8-filling) potentially interesting to stabilize new insulating phases. We study the metal-insulator transition within the extended t-J model for increasing Coulomb repulsion and we introduce then (following Ref. 12) an effective model describing the insulating state of matter. In order to characterize the various insulating phases, (i) we analyze the structure of the low-energy spectrum in the light of group theory predictions for symmetry-breaking phenomena and (ii) we compute, for the first time in the case of itinerant systems, diagonal and off-diagonal plaquette correlation functions.

Our starting point is the (fermionic) extended Hubbard-like model including nearest neighbor repulsion V on the checkerboard lattice. Here, we consider the limit where the on-site repulsion U is very large (and the largest energy scale), thus forbidding double occupancy via the Gutzwiller projector \mathcal{P}_G and leading to a

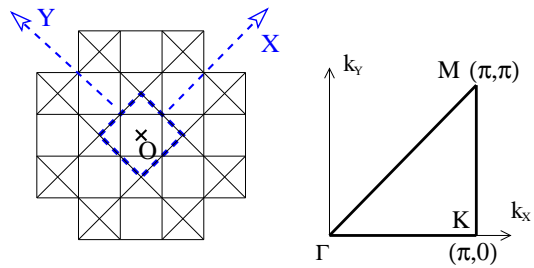


FIG. 1: (Color on-line) Left: the pyrochlore lattice is composed of “crossed plaquettes” and “empty squares”. The two-site unit cell (dashed square) and the X and Y axes considered in this study are shown. The C_{4v} point group is defined w.r.t the center O of an empty square. Right: Path $\Gamma - M - K - \Gamma$ in the first Brillouin zone considered in this study.

t-J-V model description:

$$\begin{aligned} \mathcal{H} &= -t \sum_{i,j} \mathcal{P}_G \left(c_{i\sigma}^\dagger c_{j\sigma} + h.c. \right) \mathcal{P}_G + V \sum_{i,j} n_i n_j + H_J, \\ H_J &= -J \sum_{\langle ij \rangle} \left(\frac{1}{4} - \mathbf{S}_i \cdot \mathbf{S}_j \right) n_i n_j, \end{aligned} \quad (1)$$

where J is the AF exchange constant. Hereafter, when dealing with this model and if not specified, $t = 1$ sets the energy scale. Exact Diagonalisations (ED) have been performed on a periodic $\sqrt{32} \times \sqrt{32}$ cluster ($N = 32$ sites) using full translation, point group (see Fig. 1) and time-reversal ($S_i^Z \rightarrow -S_i^Z$) symmetries¹⁴.

B. Metal-Insulator transition in the t-J-V model

In the following, we focus on the special electron densities, $n = k\frac{1}{4}$, where the integer k is 1, 2 or 3, for which we expect an insulator for sufficiently large ratio $V/|t|$. The metal-insulator (MI) transition (for increasing V) we are interested in is not directly connected to any nesting properties of the Fermi surface but it is rather induced by the Coulomb potential itself (hence it appears for both signs of t). To understand it qualitatively, let us first assume that the NN repulsion V is the largest energy scale in Hamiltonian (1). In that case, the Coulomb energy is minimized by fulfilling the “ice rule” constraint of exactly k electrons in each tetrahedra. This condition still preserves an extensive (e.g. macroscopic) manifold of states^{7,10,11,12}. Although quantum fluctuations occur between such configurations (in second order in t), the GS is an insulator since no charge can be driven between two distant locations in the system without violating the local constraints. Because of the huge (i.e. macroscopic) degeneracy of the classical problem ($V = \infty$), it is clear that the GS should be different from a simple CDW where particles are localized at fixed locations, and should exhibit a more subtle and richer nature as seen later on.

We have investigated numerically the MI transition as a function of V by computing the charge structure factor

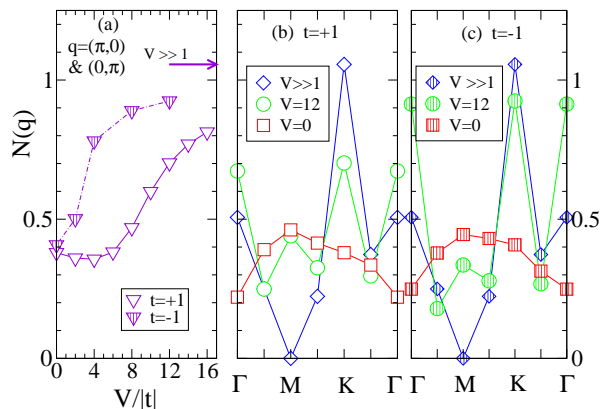


FIG. 2: (Color on-line) Density structure factor in the GS of the t-J-V model for $n = 1/4$ and $J = 0.2$ calculated by ED on a 32-site cluster. (a) Structure factor at momentum $\mathbf{q} = (\pi, 0)$ or $(0, \pi)$ vs $V/|t|$; (b,c) Structure factors as a function of momentum following the path in the BZ shown in Fig. 1. Open (dashed) symbols correspond to positive (negative) t . The points labelled as “ $V \gg 1$ ” are obtained with the effective model with $W = 0$.

$N(\mathbf{q}) = \sum_{\mathbf{R}} \exp(i\mathbf{q} \cdot \mathbf{R}) N(|\mathbf{R}|)$, the Fourier transform of the (equal-time) density-density spatial correlation at distance $R = |\mathbf{R}|$,

$$N(R) = \frac{1}{N/2} \sum_{i,j} \{ \langle n_i n_j \rangle - n^2 \}, \quad (2)$$

where the sum (over $N/2$ terms, N being the number of sites) is restricted to sites i and j such that $|\mathbf{r}_i - \mathbf{r}_j| = R$ and \mathbf{R} has *integer* coordinates in terms of the *unit cell lattice vectors* of Fig. 1 (hence i and j belong to the same sublattice). Note that the disconnected part has been subtracted for convenience. As shown in Fig. 2 for $n = 1/4$ and $J/t = 0.2$, characteristic “Bragg” peaks at $\mathbf{q} = (\pi, 0)$ and $(0, \pi)$ appear for increasing V signaling some form of charge ordering characteristic of a MI transition. However, the complexity of the insulating phase will be revealed by the simultaneous emergence of other types of correlations, such as *plaquette* correlations to be discussed later on, suggesting a more subtle and exotic GS than a simple CDW. We also note that the occurrence of a MI transition is of course independent on the sign of the hopping t . However, our data show that the rise of the Bragg peak is more abrupt for negative t and we cannot exclude the MI transition to be located at $V = 0$ in that case (which might be related to the existence of a flat band at the bottom of the tight-binding band). However the finiteness of the cluster does not enable to address the issue of the order of these transitions.

Similar behaviors are of course expected for $n = 1/2$ and $n = 3/4$ although a direct calculation with Hamiltonian (1) is beyond the power of available computers. Note however that for $t > 0$ perfect nesting of the non-interaction Fermi surface occurs at $n = 1/2$; hence an instability towards a VBC (with non-equivalent crossed

plaquettes) occurs for arbitrary small interaction¹⁵ while a different insulating phase is stabilized at larger V as discussed already in Ref. 12 and in the following sections. An Insulator-to-Insulator transition is then expected in contrast to $n = 1/4$ and $n = 3/4$ (for both signs of t) and in contrast to $n = 1/2$ with $t < 0$. In all the latter cases, a single MI transition occurs as depicted above for $n = 1/4$, a density for which a numerical calculations was feasible.

C. Effective model and mapping onto Quantum Dimer or Loop models

The ice rule constraint (in the insulator at large- V) leads to simple interesting connections to quantum fully-packed loop or dimer models⁶. Indeed, by associating to each electron a *dimer* joining the centers of the two corner-sharing tetrahedra it belongs to, a configuration at $n = 1/4$ or $n = 3/4$ ($n = 1/2$) can be represented as a dimer (loop) configuration. In contrast to bosonic analogs⁷, each dimer now carries a spin-1/2 degrees of freedom. To fully characterize the insulating phase, following Ref. 12, we consider its effective Hamiltonian acting within the constrained Hilbert space, $\mathcal{H} = H_{\square} + H_J$ with :

$$H_{\square} = -t_2 \sum_s P_{\square}(s), \quad (3)$$

$$P_{\square}(s) = \left(c_{i\uparrow}^{\dagger} c_{j\downarrow}^{\dagger} - c_{i\downarrow}^{\dagger} c_{j\uparrow}^{\dagger} \right) \left(c_{k\downarrow} c_{l\uparrow} - c_{k\uparrow} c_{l\downarrow} \right) + \left(c_{k\uparrow}^{\dagger} c_{l\downarrow}^{\dagger} - c_{k\downarrow}^{\dagger} c_{l\uparrow}^{\dagger} \right) \left(c_{i\downarrow} c_{j\uparrow} - c_{i\uparrow} c_{j\downarrow} \right) \quad (4)$$

where $t_2 = \frac{2t^2}{V}$ and the summation is over the void plaquettes labelled by s of the checkerboard lattice. The sites of s are ordered as i, k, j and l in the clockwise (or anti-clockwise) direction. $P_{\square}(s)$ is a second-order process which preserves the ice rule. It acts on two electrons forming a singlet bond on one of the two diagonals of s , and rotates the bond by 90° degree.

D. Description of the expected ordered phases

The kinetic processes of Eq. (3) favor singlet electron pairs resonating on void plaquettes (empty squares) and could lead to long-range plaquette-plaquette correlations. Fig. 3(a) shows pictorially the expected Resonant Singlet Pair Crystals exhibiting such a plaquette ordering. For $n = 1/2$ it was indeed shown that the $\mathbf{q} = (\pi, \pi)$ RSPC is stable¹² as long as $J/t_2 < 1.5$. Note that the GS of the RSPC is two-fold degenerate at $n = 1/2$ while one expects a four-fold degenerate GS at $n = 1/4$ and $n = 3/4$ in connection with $\mathbf{q} = (\pi, \pi)$, $(\pi, 0)$ and $(0, \pi)$ plaquette order as seen later. In addition, the average charge density of the $n = 1/2$ RSPC is uniform while $\mathbf{q} = (\pi, 0)$ and $(0, \pi)$ (charge density) Bragg peaks should be present at $n = 1/4$ and $n = 3/4$ consistently with the

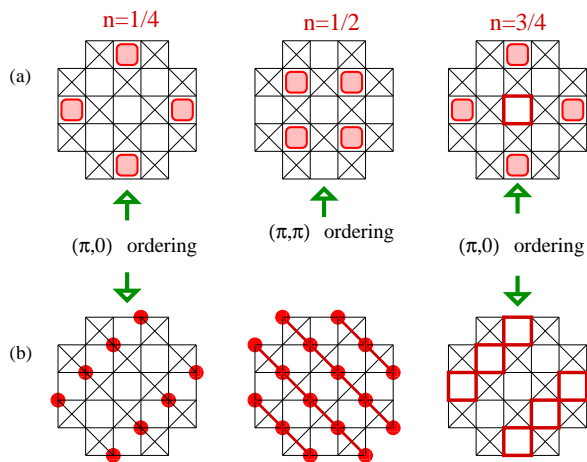


FIG. 3: (Color on-line) Schematic views of the plaquette (a) and columnar (b) phases considered in this work for electron densities $n = 1/4$, $1/2$ and $3/4$ (as shown). Dots, shaded plaquettes and (red) thick lines correspond to electrons, singlet pairs resonating on a plaquette and AF bonds, respectively.

charge ordering observed previously at the MI transition. However, a full characterization of the insulating phases is delicate since the RSPC of Fig. 3(a) in fact compete with the columnar-like phases of Fig. 3(b) which optimize the numbers of possible t2- (or dimer-) flips. For $n = 1/4$ and $n = 3/4$ both RSPC and columnar phases exhibit $(\pi, 0)$ and $(0, \pi)$ plaquette (and charge) ordering as shown later. However, at $n = 1/2$, only the RSPC exhibits (π, π) plaquette ordering. Similarly, only the columnar states break rotation symmetry (for all commensurate densities).

The various candidate phases hence correspond to different symmetry-breaking phenomena which should be directly reflected in the structure of the low-energy spectra. Table I summarizes the quantum numbers of the quasi-degenerate states which should collapse onto the GS in the thermodynamic limit. Indeed, from linear combinations of all the equivalent translated and/or rotated patterns obtained from each of the representative ones in Fig. 3, one can easily build the (orthogonal) states carrying the appropriate quantum numbers reported in Table I. Analyzing the low-energy energy spectra should then give clear signals on the nature of the symmetry-breaking phase.

E. Analysis of the low-energy spectra: hints for symmetry-breaking GS

Prior to the detailed analysis of the low-energy spectra it is useful to carry on the connection to the usual Quantum Dimer Model (QDM)⁶ and, following Ref. 12, add to $\tilde{\mathcal{H}}$ a “diagonal” term corresponding to the 4-site

Ordered Phase	$(0, 0)$ A_1	$(0, 0)$ B_1	(π, π) A_1	$(\pi, 0)$ A_1	$(\pi, 0)$ A_1 (*)	(π, π) B_1
$n = 1/2$ RSPC	X		X			
$n = 1/2$ Colum.	X	X				
$n = 1/4, 3/4$ RSPC	X		X	X		
$n = 1/4, 3/4$ Colum.	X	X		X		
$n = 1/4, 3/4$ Mixed	X	X	X	X	X	X

TABLE I: Quantum numbers of the degenerate GS of the various ordered phases considered here. Note that momentum $(\pi, 0)$ is degenerate with $(0, \pi)$ (not shown). Standard notations are used to denote the irreducible representations of the C_{4v} (C_{2v}) point group (acting around point O in Fig. 1) for momentum $(0, 0)$ and (π, π) ($(\pi, 0)$). (*) stands for a *second* $\{(\pi, 0), A_1\}$ state. The RSPC, columnar and mixed GS are 2-, 4- and 8-fold degenerate respectively.

ring exchange:

$$\mathcal{H}_W = W \sum_{\square} \left[\left(\frac{1}{2} - 2\mathbf{S}_i \cdot \mathbf{S}_j \right) n_i n_j (1 - n_l)(1 - n_k) + \left(\frac{1}{2} - 2\mathbf{S}_k \cdot \mathbf{S}_l \right) n_k n_l (1 - n_i)(1 - n_j) \right], \quad (5)$$

the summation is again over the empty squares $s = (i, k, j, l)$ and the notations are the same as in Eq. (3). The Hamiltonian at the Rohrsar-Kivelson point (i.e. for $W = t_2$)^{6,12} is a sum of projectors. Although our original problem corresponds to $W = 0$, analyzing the evolution of the system from large negative W value (for which a columnar phase is stabilized) up to the RK point offers new insights to characterize the $W = 0$ phase (we shall not consider here the case $W > t_2$ where localized states are stabilized). This strategy has been applied successfully in Ref. 12 for $n = 1/2$ and we extend it here to the more complex $n = 1/4$ and $n = 3/4$ cases. Fig. 4 shows the low-energy spectra vs W/t_2 for all three commensurate electron densities considered here. For $n = 1/2$ and $n = 3/4$, increasing W from negative value upwards, a level crossing is found around $W/t_2 = w_c \simeq -1.2$ signaling a (possibly first-order) phase transition. Indeed, our results in Fig. 4(b,c) compared to the GS degeneracy of the ordered states listed in Table I strongly suggest that the columnar phase (the RSPC) is stable for $W/t_2 < w_c$ ($W/t_2 > w_c$) since a group of two or four quasi-degenerate states (with exactly the expected quantum numbers) separated from the rest of the spectrum by a small gap can clearly be identified. In contrast, no level crossing occurs for $n = 1/4$ so that no conclusion can be drawn yet for this case (the 8-fold degenerate “mixed” state of Table I not being completely excluded at this point). For $n = 1/2$ and $n = 3/4$, the “physical points” $W = 0$ are clearly located in the region of stability of the RSPC.

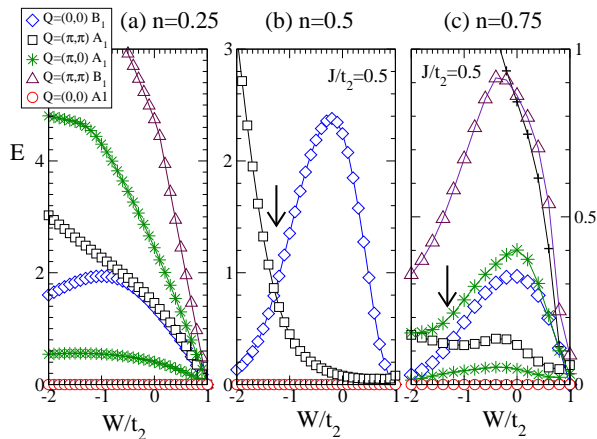


FIG. 4: (Color on-line) Lowest excitations (w.r.t. the GS energy) vs W/t_2 for $n = 1/4$, (a) $1/2$ (b) and $3/4$ (c) obtained by ED of a 32-site cluster. Different symbols correspond to different irreducible representations as shown in the legend. Other excitations (+ symbols in (c)) have significantly higher energies. In (b) and (c) the vertical arrows indicate the level crossings between the $\{(0,0), B_1\}$ and $\{(\pi,\pi), A_1\}$ states characteristic of the columnar state and the RSPC respectively.

F. Off-diagonal plaquette-exchange correlation function

In order to get complementary fingerprints associated to a given type of symmetry-breaking and more insights on the nature of the insulating phases, it is of interest to compute the plaquette-exchange structure factor $C_{\text{pl}}(\mathbf{q}) = \sum_{\mathbf{R}} \exp(i\mathbf{q} \cdot \mathbf{R}) C_{\text{pl}}(|\mathbf{R}|)$, the Fourier transform of the spatial plaquette correlations at distance $R = |\mathbf{R}|$,

$$C_{\text{pl}}(R) = \frac{1}{N/2} \sum_{s,s'} \{ \langle P_{\square}(s) P_{\square}(s') \rangle - \langle P_{\square}(s) \rangle \langle P_{\square}(s') \rangle \}, \quad (6)$$

where the sum is restricted to plaquettes such that $|\mathbf{R}_s - \mathbf{R}_{s'}| = R$ and we have again subtracted the disconnected part. Despite the intrinsic complexity of computing a 8-fermion correlator, the implementation is made easier by the fact that the operator to average has the full translation and rotation symmetry of the lattice.

We have first studied the emergence of superstructure peaks in the plaquette structure factor on the original t-J-V model itself and the results at $1/8$ -filling are shown in Fig. 5. For $V = 0$ the correlations have no structure in momentum space. However, for increasing V , superstructure peaks at momenta $(\pi, 0)$ and $(0, \pi)$ (as well as harmonics at (π, π)) clearly develop. The behavior of the $(\pi, 0)$ peak with V follows quite faithfully the behavior of the “charge” Bragg peak of Fig. 2 indicating that charge and plaquette orderings seem to be tightly connected.

Next, we turn to the case of the effective model describing the insulating phase and results are shown in Fig. 6. At quarter-filling ($n = 1/2$), the large peak emerging at

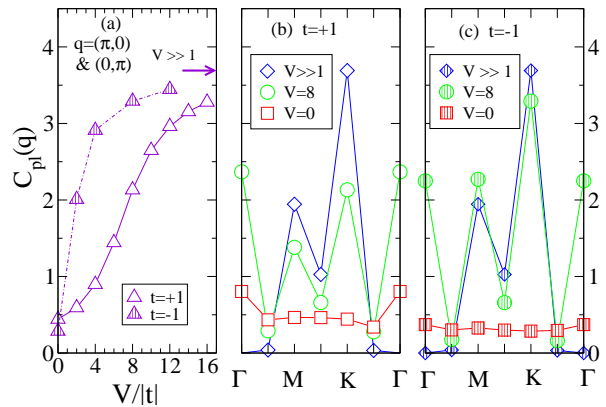


FIG. 5: (Color on-line) Plaquette-exchange structure factor in the GS of the t-J-V model for $n = 1/4$ and $J = 0.2$ obtained by ED of a 32-site cluster. (a) Structure factor at momentum $\mathbf{q} = (\pi, 0)$ or $(0, \pi)$ vs $V/|t|$; (b,c) Structure factor as a function of momentum following the path in the BZ shown in Fig. 1. Open (dashed) symbols correspond to positive (negative) t . The points labeled as “ $V \gg 1$ ” are obtained with the effective model with $W = 0$.

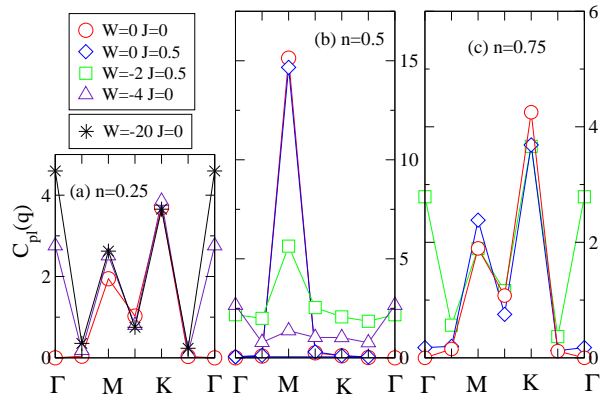


FIG. 6: (Color on-line) Plaquette-exchange structure factors in the GS of the effective $t_2 - J - W$ model vs momentum \mathbf{q} along the path shown in Fig. 1 and for different choices of W and J as indicated in the legend (in units of t_2). (a), (b) and (c) correspond to commensurate fillings $n = 0.25$, $n = 0.5$ and $n = 0.75$, respectively. Results are obtained by ED of a 32-site cluster.

(π, π) is directly linked to the existence of the RSPC (at $W = 0$) while it is suppressed in the columnar phase at sufficiently negative W values, $W/t_2 < w_c$, where translation symmetry is restored. On the contrary, for $n = 1/4$ and $3/4$, since both columnar and RSPC phases break translation symmetry superstructure peaks at momenta $(\pi, 0)$, $(0, \pi)$ and (π, π) are always present irrespective of the value of W .

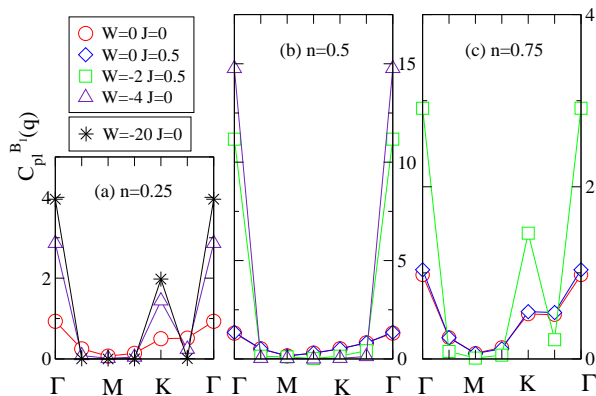


FIG. 7: (Color on-line) B_1 -plaquette structure factors in the GS of the effective $t_2 - J - W$ model vs momentum \mathbf{q} along the path shown in Fig. 1. Same parameters and notations as Fig. 6.

G. Diagonal B_1 -plaquette correlation function: hints for rotational symmetry breaking

The analysis of the low-energy spectrum strongly suggests a transition from the columnar phase to the RSPC by varying W , at least for $n = 1/2$ and $n = 3/4$. We therefore expect to be able to detect directly the signal of the columnar order via the emergence of some long-range correlations. Note that the above investigation of the plaquette-exchange structure factor, by detecting lattice translation symmetry breaking, was able to discriminate between columnar and RSPC phases only for $n = 1/2$. Since the rotational symmetry-breaking in the columnar phase is achieved via the collapse of a $\{\mathbf{q} = \mathbf{0}, B_1\}$ state onto the GS in the thermodynamic limit, it is natural to define a diagonal B_1 -plaquette correlator as,

$$C_{\text{pl}}^{B_1}(R) = \frac{1}{N/2} \sum_{s,s'}^l \langle P_{\square}^{B_1}(s) P_{\square}^{B_1}(s') \rangle, \quad (7)$$

with the diagonal plaquette operator defined as,

$$P_{\square}^{B_1}(s) = n_i n_j - n_k n_l, \quad (8)$$

and the rest of the notations is the same as in Eqs. (3) and 6. Note that there is no need here to subtract the disconnected part since it is vanishing for obvious symmetry reasons.

The results for the related plaquette structure factor (defined as before) vs momentum are shown in Fig. 7 and clearly reveal the appearance of a strong $\mathbf{q} = \mathbf{0}$ peak (with an additional peak at (π, π) for $n = 1/4$ and $n = 3/4$) in the columnar phase i.e. for sufficiently negative W values, $W/t_2 < w_c$. In contrast, for $W = 0$, which is the case relevant to the original t - J - V model, the B_1 -plaquette structure factor remains very flat in momentum space consistently with the existence of a rotationally-symmetric RSPC for all three values of the densities studied here. This clearly confirms our previous

results for $n = 1/2$ and $n = 3/4$ and suggests strongly that the case $n = 1/4$ is similar. We therefore attribute the lack of level crossing in the previous spectral analysis for $n = 1/4$ to a finite size effect.

H. Comparison to the bosonic case

It is of interest to compare our results to the bosonic system (again with infinite on-site repulsion and large NN repulsion) whose effective Hamiltonian is given by (3) where $P_{\square}(s)$ is now replaced by $P_{\square}(s) = b_i^\dagger b_j^\dagger b_k b_l$ in terms of the usual *hard-core* boson creation and annihilation operators on the empty square (i, j, k, l) . For $n = 1/2$ the bosonic system can be mapped on the usual fully-packed quantum loop model (or a quantized six-vertex model) with only kinetic processes (i.e. $W = 0$) exhibiting a plaquette phase⁷ bearing some similarities with the fermionic RSPC¹². However, the stability of the plaquette phase w.r.t. additional parameters (e.g. W) is more fragile for bosons. The $n = 1/4$ and $n = 3/4$ cases reduce, for bosons, to the usual QDM⁶ studied recently by extensive QMC methods¹⁶ and believed to have a columnar GS in the absence of diagonal interactions (i.e. $W = 0$). This is different from our results for spinful fermions exhibiting a rotationally-invariant RSPC GS. This emphasizes the special role of the spin degrees of freedom in stabilizing plaquette phases. Note however that Ref. 5 reports for the hard-core bosons system at $n = 1/4$, increasing the NN V , a MI transition at $V/t \sim 3.2$ towards a *plaquette* phase different from the supposed GS in the $V/t \gg 1$ limit described by the QDM¹⁶. The evolution from the MI point to larger V needs certainly to be clarified.

I. Conclusions

To summarize, using a t - J model extended with NN Coulomb repulsion, the metal-insulator transition has been investigated on the planar pyrochlore frustrated lattice at 1/8-filling (i.e. $n = 1/4$), a tractable case numerically. For increasing repulsion, the emergence of superstructure (charge) Bragg peaks signals the onset of the insulating phase which also immediately develops some form of plaquette ordering. To understand further the complex nature of the insulating phase, an effective model valid for commensurate fillings like $n = 1/4$, $n = 1/2$ and $n = 3/4$ and in the limit of large NN repulsion is used. Remarkably, the frustrated nature of the lattice leads then to ice rule-like constraints so that the Hilbert space can be mapped onto a manifold of fully-packed dimer or loop coverings with extra spin degrees of freedom. Quantum fluctuations take the form of simple (second-order) kinetic processes that bear strong resemblance with the usual bosonic QDM. Among the various type of lattice symmetry-breaking states, several compelling evidences are given in favor of a plaquette GS, the RSPC. This new state of matter introduced earlier

in the quarter-filled case¹², is extended here to 1/8 and 3/8 fillings for which it has a twice larger supercell and a twice larger GS degeneracy. A detailed analysis of the low-energy spectra supplemented by symmetry considerations as well as the calculation of several types of *plaquette* correlations support our claims. To carry on the analogy with the QDM, following Ref. 12, we also introduced a diagonal plaquette interaction and showed signatures of a (presumably first order) transition towards a columnar phase as this parameter is tuned to more negative values.

J. Acknowledgements

I thank the *Agence Nationale de la Recherche* (France) for support, IDRIS (Orsay, France) for computer time and the Theoretical Physics laboratory at ETH-Zürich for warm hospitality. I am also happy to thank Manfred Sigrist and Matthias Troyer for valuable discussions and I am indebted to Karlo Penc and Nic Shannon for patiently explaining basic ideas and (eventually) getting me interested in this problem.

-
- ¹ G. Misguich and C. Lhuillier, p. 229, in “Frustrated Spin Systems”, Eds. H.T. Diep, World Scientific (Singapore, 2004).
- ² J.-B. Fouet, M. Mambrini, P. Sindzingre, and C. Lhuillier, Phys. Rev. B **67**, 054411 (2003); A similar plaquette phase has also been found on the simple square lattice when next-next-NN AF interactions are included: M. Mambrini, A. Läuchli, D. Poilblanc and F. Mila, Phys. Rev. B **74**, 144422 (2006).
- ³ A. Läuchli and D. Poilblanc, Phys. Rev. Lett. **92**, 236404 (2004); D. Poilblanc, Phys. Rev. Lett. **93**, 197204 (2004).
- ⁴ S. Wessel and M. Troyer, Phys. Rev. Lett. **95**, 127205 (2005); D. Heidarian and K. Damle, Phys. Rev. Lett. **95**, 127206 (2005); R.G. Melko, A. Paramekanti, A.A. Burkov, A. Vishwanath, D.N. Sheng, and L. Balents Phys. Rev. Lett. **95**, 127207 (2005).
- ⁵ Arnab Sen, Kedar Damle and T. Senthil, cond-mat/0701476.
- ⁶ D.S. Rokhsar and S.A. Kivelson, Phys. Rev. Lett. **61**, 2376 (1988).
- ⁷ N. Shannon, G. Misguich, K. Penc, Phys. Rev. B **69**, 220403(R) (2004); these authors use the “spin language” and consider the anisotropic XXZ Heisenberg model. Large anisotropy corresponds to large NN repulsion between bosons. Note that plaquette ordering survives up to the SU(2)-symmetric point of Ref. 2.
- ⁸ The Hilbert space can also be mapped onto the configuration space of a 6-vertex model: E.H. Lieb, Phys. Rev. Lett. **18**, 1046 (1967).
- ⁹ Karlo Penc, unpublished.
- ¹⁰ F. Pollmann, J.J. Betouras, K. Shtengel, and P. Fulde, Phys. Rev. Lett. **97**, 170407 (2006); F. Pollmann, P. Fulde, and E. Runge, Phys. Rev. B **73**, 125121 (2006).
- ¹¹ P. Fulde, K. Penc and N. Shannon, Annalen der Physik, **11**, 892 (2002).
- ¹² D. Poilblanc, K. Penc and N. Shannon, cond-mat/0702367.
- ¹³ H.P. Büchler et al., Phys. Rev. Lett. **95**, 040402 (2005) and references therein.
- ¹⁴ The largest Hilbert space was obtained for $n = 3/4$ and $\{(\pi, 0), A_1\}$ symmetry (5,757,416 symmetrized states).
- ¹⁵ M. Indergand, C. Honerkamp, A. Läuchli, D. Poilblanc and M. Sigrist, Phys. Rev. B **75**, 045105 (2007).
- ¹⁶ O. Syljuasen, Phys. Rev. B **73**, 245105 (2006).